

Observation of a new charmonium state in double charmonium production in e^+e^- annihilation at $\sqrt{s} \approx 10.6$ GeV

K. Abe,⁹ K. Abe,⁴⁷ I. Adachi,⁹ H. Aihara,⁴⁹ K. Aoki,²³ K. Arinstein,² Y. Asano,⁵⁴
 T. Aso,⁵³ V. Aulchenko,² T. Aushev,¹³ T. Aziz,⁴⁵ S. Bahinipati,⁵ A. M. Bakich,⁴⁴
 V. Balagura,¹³ Y. Ban,³⁶ S. Banerjee,⁴⁵ E. Barberio,²² M. Barbero,⁸ A. Bay,¹⁹ I. Bedny,²
 U. Bitenc,¹⁴ I. Bizjak,¹⁴ S. Blyth,²⁵ A. Bondar,² A. Bozek,²⁹ M. Bračko,^{9, 21, 14}
 J. Brodzicka,²⁹ T. E. Browder,⁸ M.-C. Chang,⁴⁸ P. Chang,²⁸ Y. Chao,²⁸ A. Chen,²⁵
 K.-F. Chen,²⁸ W. T. Chen,²⁵ B. G. Cheon,⁴ C.-C. Chiang,²⁸ R. Chistov,¹³ S.-K. Choi,⁷
 Y. Choi,⁴³ Y. K. Choi,⁴³ A. Chuvikov,³⁷ S. Cole,⁴⁴ J. Dalseno,²² M. Danilov,¹³ M. Dash,⁵⁶
 L. Y. Dong,¹¹ R. Dowd,²² J. Dragic,⁹ A. Drutskoy,⁵ S. Eidelman,² Y. Enari,²³ D. Epifanov,²
 F. Fang,⁸ S. Fratina,¹⁴ H. Fujii,⁹ N. Gabyshev,² A. Garmash,³⁷ T. Gershon,⁹ A. Go,²⁵
 G. Gokhroo,⁴⁵ P. Goldenzweig,⁵ B. Golob,^{20, 14} A. Gorišek,¹⁴ M. Grosse Perdekamp,³⁸
 H. Guler,⁸ R. Guo,²⁶ J. Haba,⁹ K. Hara,⁹ T. Hara,³⁴ Y. Hasegawa,⁴² N. C. Hastings,⁴⁹
 K. Hasuko,³⁸ K. Hayasaka,²³ H. Hayashii,²⁴ M. Hazumi,⁹ T. Higuchi,⁹ L. Hinz,¹⁹ T. Hojo,³⁴
 T. Hokuue,²³ Y. Hoshi,⁴⁷ K. Hoshina,⁵² S. Hou,²⁵ W.-S. Hou,²⁸ Y. B. Hsiung,²⁸
 Y. Igarashi,⁹ T. Iijima,²³ K. Ikado,²³ A. Imoto,²⁴ K. Inami,²³ A. Ishikawa,⁹ H. Ishino,⁵⁰
 K. Itoh,⁴⁹ R. Itoh,⁹ M. Iwasaki,⁴⁹ Y. Iwasaki,⁹ C. Jacoby,¹⁹ C.-M. Jen,²⁸ R. Kagan,¹³
 H. Kakuno,⁴⁹ J. H. Kang,⁵⁷ J. S. Kang,¹⁶ P. Kapusta,²⁹ S. U. Kataoka,²⁴ N. Katayama,⁹
 H. Kawai,³ N. Kawamura,¹ T. Kawasaki,³¹ S. Kazi,⁵ N. Kent,⁸ H. R. Khan,⁵⁰
 A. Kibayashi,⁵⁰ H. Kichimi,⁹ H. J. Kim,¹⁸ H. O. Kim,⁴³ J. H. Kim,⁴³ S. K. Kim,⁴¹
 S. M. Kim,⁴³ T. H. Kim,⁵⁷ K. Kinoshita,⁵ N. Kishimoto,²³ S. Korpar,^{21, 14} Y. Kozakai,²³
 P. Križan,^{20, 14} P. Krokovny,⁹ T. Kubota,²³ R. Kulasiri,⁵ C. C. Kuo,²⁵ H. Kurashiro,⁵⁰
 E. Kurihara,³ A. Kusaka,⁴⁹ A. Kuzmin,² Y.-J. Kwon,⁵⁷ J. S. Lange,⁶ G. Leder,¹²
 S. E. Lee,⁴¹ Y.-J. Lee,²⁸ T. Lesiak,²⁹ J. Li,⁴⁰ A. Limosani,⁹ S.-W. Lin,²⁸ D. Liventsev,¹³
 J. MacNaughton,¹² G. Majumder,⁴⁵ F. Mandl,¹² D. Marlow,³⁷ H. Matsumoto,³¹
 T. Matsumoto,⁵¹ A. Matyja,²⁹ Y. Mikami,⁴⁸ W. Mitaroff,¹² K. Miyabayashi,²⁴ H. Miyake,³⁴
 H. Miyata,³¹ Y. Miyazaki,²³ R. Mizuk,¹³ D. Mohapatra,⁵⁶ G. R. Moloney,²² T. Mori,⁵⁰
 A. Murakami,³⁹ T. Nagamine,⁴⁸ Y. Nagasaka,¹⁰ T. Nakagawa,⁵¹ I. Nakamura,⁹
 E. Nakano,³³ M. Nakao,⁹ H. Nakazawa,⁹ Z. Natkaniec,²⁹ K. Neichi,⁴⁷ S. Nishida,⁹
 O. Nitoh,⁵² S. Noguchi,²⁴ T. Nozaki,⁹ A. Ogawa,³⁸ S. Ogawa,⁴⁶ T. Ohshima,²³ T. Okabe,²³
 S. Okuno,¹⁵ S. L. Olsen,⁸ Y. Onuki,³¹ W. Ostrowicz,²⁹ H. Ozaki,⁹ P. Pakhlov,¹³ H. Palka,²⁹
 C. W. Park,⁴³ H. Park,¹⁸ K. S. Park,⁴³ N. Parslow,⁴⁴ L. S. Peak,⁴⁴ M. Pernicka,¹²
 R. Pestotnik,¹⁴ M. Peters,⁸ L. E. Piilonen,⁵⁶ A. Poluektov,² F. J. Ronga,⁹ N. Root,²
 M. Rozanska,²⁹ H. Sahoo,⁸ M. Saigo,⁴⁸ S. Saitoh,⁹ Y. Sakai,⁹ H. Sakamoto,¹⁷
 H. Sakaue,³³ T. R. Sarangi,⁹ M. Satapathy,⁵⁵ N. Sato,²³ N. Satoyama,⁴² T. Schietinger,¹⁹
 O. Schneider,¹⁹ P. Schönmeier,⁴⁸ J. Schümann,²⁸ C. Schwanda,¹² A. J. Schwartz,⁵
 T. Seki,⁵¹ K. Senyo,²³ R. Seuster,⁸ M. E. Sevior,²² T. Shibata,³¹ H. Shibuya,⁴⁶
 J.-G. Shiu,²⁸ B. Shwartz,² V. Sidorov,² J. B. Singh,³⁵ A. Somov,⁵ N. Soni,³⁵ R. Stamen,⁹
 S. Stanič,³² M. Starič,¹⁴ A. Sugiyama,³⁹ K. Sumisawa,⁹ T. Sumiyoshi,⁵¹ S. Suzuki,³⁹
 S. Y. Suzuki,⁹ O. Tajima,⁹ N. Takada,⁴² F. Takasaki,⁹ K. Tamai,⁹ N. Tamura,³¹
 K. Tanabe,⁴⁹ M. Tanaka,⁹ G. N. Taylor,²² Y. Teramoto,³³ X. C. Tian,³⁶ K. Trabelsi,⁸

Y. F. Tse,²² T. Tsuboyama,⁹ T. Tsukamoto,⁹ K. Uchida,⁸ Y. Uchida,⁹ S. Uehara,⁹ T. Uglov,¹³ K. Ueno,²⁸ Y. Unno,⁹ S. Uno,⁹ P. Urquijo,²² Y. Ushiroda,⁹ G. Varner,⁸ K. E. Varvell,⁴⁴ S. Villa,¹⁹ C. C. Wang,²⁸ C. H. Wang,²⁷ M.-Z. Wang,²⁸ M. Watanabe,³¹ Y. Watanabe,⁵⁰ L. Widhalm,¹² C.-H. Wu,²⁸ Q. L. Xie,¹¹ B. D. Yabsley,⁵⁶ A. Yamaguchi,⁴⁸ H. Yamamoto,⁴⁸ S. Yamamoto,⁵¹ Y. Yamashita,³⁰ M. Yamauchi,⁹ Heyoung Yang,⁴¹ J. Ying,³⁶ S. Yoshino,²³ Y. Yuan,¹¹ Y. Yusa,⁴⁸ H. Yuta,¹ S. L. Zang,¹¹ C. C. Zhang,¹¹ J. Zhang,⁹ L. M. Zhang,⁴⁰ Z. P. Zhang,⁴⁰ V. Zhilich,² T. Ziegler,³⁷ and D. Zürcher¹⁹

(The Belle Collaboration)

¹*Aomori University, Aomori*

²*Budker Institute of Nuclear Physics, Novosibirsk*

³*Chiba University, Chiba*

⁴*Chonnam National University, Kwangju*

⁵*University of Cincinnati, Cincinnati, Ohio 45221*

⁶*University of Frankfurt, Frankfurt*

⁷*Gyeongsang National University, Chinju*

⁸*University of Hawaii, Honolulu, Hawaii 96822*

⁹*High Energy Accelerator Research Organization (KEK), Tsukuba*

¹⁰*Hiroshima Institute of Technology, Hiroshima*

¹¹*Institute of High Energy Physics,*

Chinese Academy of Sciences, Beijing

¹²*Institute of High Energy Physics, Vienna*

¹³*Institute for Theoretical and Experimental Physics, Moscow*

¹⁴*J. Stefan Institute, Ljubljana*

¹⁵*Kanagawa University, Yokohama*

¹⁶*Korea University, Seoul*

¹⁷*Kyoto University, Kyoto*

¹⁸*Kyungpook National University, Taegu*

¹⁹*Swiss Federal Institute of Technology of Lausanne, EPFL, Lausanne*

²⁰*University of Ljubljana, Ljubljana*

²¹*University of Maribor, Maribor*

²²*University of Melbourne, Victoria*

²³*Nagoya University, Nagoya*

²⁴*Nara Women's University, Nara*

²⁵*National Central University, Chung-li*

²⁶*National Kaohsiung Normal University, Kaohsiung*

²⁷*National United University, Miao Li*

²⁸*Department of Physics, National Taiwan University, Taipei*

²⁹*H. Niewodniczanski Institute of Nuclear Physics, Krakow*

³⁰*Nippon Dental University, Niigata*

³¹*Niigata University, Niigata*

³²*Nova Gorica Polytechnic, Nova Gorica*

³³*Osaka City University, Osaka*

³⁴*Osaka University, Osaka*

³⁵*Panjab University, Chandigarh*

³⁶*Peking University, Beijing*

³⁷*Princeton University, Princeton, New Jersey 08544*

³⁸*RIKEN BNL Research Center, Upton, New York 11973*

³⁹*Saga University, Saga*

⁴⁰*University of Science and Technology of China, Hefei*

⁴¹*Seoul National University, Seoul*

⁴²*Shinshu University, Nagano*

⁴³*Sungkyunkwan University, Suwon*

⁴⁴*University of Sydney, Sydney NSW*

⁴⁵*Tata Institute of Fundamental Research, Bombay*

⁴⁶*Toho University, Funabashi*

⁴⁷*Tohoku Gakuin University, Tagajo*

⁴⁸*Tohoku University, Sendai*

⁴⁹*Department of Physics, University of Tokyo, Tokyo*

⁵⁰*Tokyo Institute of Technology, Tokyo*

⁵¹*Tokyo Metropolitan University, Tokyo*

⁵²*Tokyo University of Agriculture and Technology, Tokyo*

⁵³*Toyama National College of Maritime Technology, Toyama*

⁵⁴*University of Tsukuba, Tsukuba*

⁵⁵*Utkal University, Bhubaneswar*

⁵⁶*Virginia Polytechnic Institute and State University, Blacksburg, Virginia 24061*

⁵⁷*Yonsei University, Seoul*

Abstract

We report the first observation of a new charmonium state at a mass of $(3.943 \pm 0.006 \pm 0.006) \text{ GeV}/c^2$. This state, called $X(3940)$, is observed in the process $e^+e^- \rightarrow J/\psi X(3940)$ in the spectrum of masses recoiling against a reconstructed J/ψ . We also observe the decay of the $X(3940)$ into $D^*\overline{D}$ and measure the intrinsic width of this state to be less than $52 \text{ MeV}/c^2$ at the 90% C.L. These results are obtained from a 350 fb^{-1} data sample collected with the Belle detector near the $\Upsilon(4S)$ resonance, at the KEKB asymmetric energy e^+e^- collider.

PACS numbers: 13.66.Bc, 12.38.Bx, 14.40.Gx

Recently there have been a number of reports of new charmonium or charmonium-like states [1, 2, 3]. One of the most intriguing puzzles is the nature of the charmonium-like state $X(3872)$ decaying into $J/\psi\pi^+\pi^-$ and observed by Belle in B decays [2]. This state has many exotic properties (see *e.g.* [4]) and so far has not been assigned to any charmonium state in the conventional quark model. This has led to speculations that $X(3872)$ might be a molecule-like weakly bound state. Even more exotic is the state observed recently in the $J/\psi\omega$ final state at a mass of around $3.94\text{ GeV}/c^2$ [3]. This latter state is above $D^*\overline{D}$ threshold but has not been found in the $D\overline{D}$ or in $D^*\overline{D}$ final states. In addition, charmonium production in different processes is not completely understood. One striking example is double charmonium production in e^+e^- annihilation observed by Belle [5] with a surprisingly large cross section. These experimental results have renewed theoretical interest in the spectroscopy, decays and production of charmonium.

In this paper we report the observation of a new charmonium state above $D\overline{D}$ threshold, $X(3940)$, produced in the process $e^+e^- \rightarrow J/\psi X(3940)$. We also search for the decay of $X(3940)$ into $D\overline{D}$, $D^*\overline{D}$ and $J/\psi\omega$. The integrated luminosity used for this analysis is 350 fb^{-1} collected by the Belle detector at the $\Upsilon(4S)$ resonance and nearby continuum at the KEKB asymmetric energy e^+e^- collider.

The J/ψ reconstruction procedure is identical to our previous published analyses [5, 6]. Oppositely charged tracks that are positively identified as muons or electrons are used for $J/\psi \rightarrow \ell^+\ell^-$ reconstruction. A partial correction for final state radiation and bremsstrahlung energy loss is performed by including the four-momentum of every photon detected within a 50 mrad cone around the electron direction in the e^+e^- invariant mass calculation. The two lepton candidate tracks are required to have a common vertex, with a distance from the interaction point in the plane perpendicular to the beam axis smaller than 1 mm. The $J/\psi \rightarrow \ell^+\ell^-$ signal region is defined by the mass window $|M_{\ell^+\ell^-} - M_{J/\psi}| < 30\text{ MeV}/c^2$ ($\approx 2.5\sigma$). J/ψ candidates in the signal window are subjected to a mass and vertex constrained fit to improve their momentum resolution.

QED processes are significantly suppressed by requiring the total charged multiplicity (N_{ch}) in the event be greater than 4. Background due to J/ψ mesons produced from $B\overline{B}$ events is removed by requiring the center-of-mass (CM) momentum $p_{J/\psi}^*$ to be greater than $2.0\text{ GeV}/c$. As in the previous analysis we define the recoil mass as

$$M_{\text{recoil}}(J/\psi) = \sqrt{(E_{\text{CMS}} - E_{J/\psi}^*)^2 - p_{J/\psi}^{*2}}, \quad (1)$$

where $E_{J/\psi}^*$ is the J/ψ CM energy after the mass constraint.

For the study of the $X(3940)$ we reconstruct D^0 candidates using five decay modes: $K^-\pi^+$, K^-K^+ , $K^-\pi^-\pi^+\pi^+$, $K_S\pi^+\pi^-$ and $K^-\pi^+\pi^0$. D^+ candidates are reconstructed using three decay modes: $K^-\pi^+\pi^+$, $K^-K^+\pi^+$ and $K_S\pi^+$. For the $D^0 \rightarrow K^-\pi^-\pi^+\pi^+$ and $D^0 \rightarrow K^-\pi^+\pi^0$ modes mass windows of $\pm 10\text{ MeV}/c^2$ and $\pm 20\text{ MeV}/c^2$ are used. A $\pm 15\text{ MeV}/c^2$ mass window is used for all other modes (approximately 2.5σ in each case). To improve their momentum resolution D candidates are refitted to the nominal D^0 or D^+ masses. To study the contribution of combinatorial background under the D peak, we use D sidebands selected from a mass window 4 times larger. Candidate ω mesons are reconstructed from $\pi^+\pi^-\pi^0$ combinations with invariant masses within a $\pm 20\text{ MeV}/c^2$ window (corresponding to $2.5\Gamma_\omega$ or 2.5σ) around the nominal ω mass. The ω sideband region is defined by $30 < |M(\pi^+\pi^-\pi^0) - M_\omega| < 50\text{ MeV}/c^2$.

The recoil mass spectrum for the data is shown in Fig. 1. In this analysis the studied recoil mass interval is extended above $D\overline{D}$ threshold; in addition to the three previously

observed peaks, another significant peak can be seen around a mass of $3.94 \text{ GeV}/c^2$. We

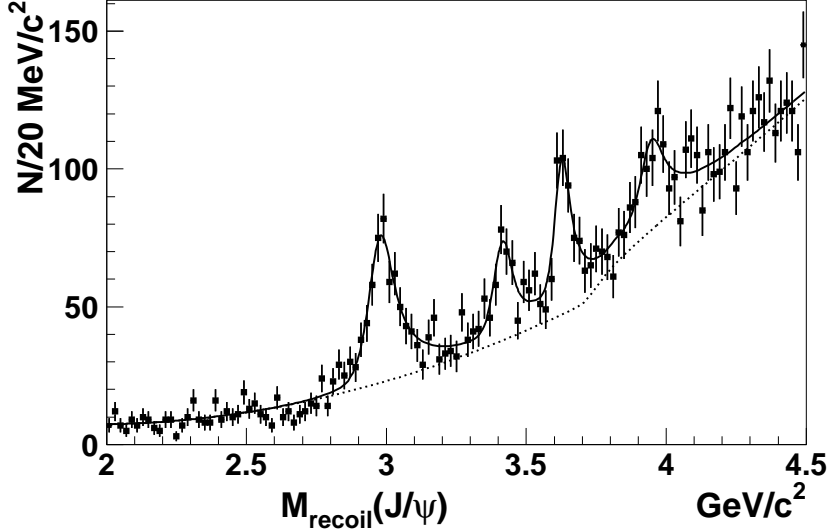


FIG. 1: The distribution of masses recoiling against the reconstructed J/ψ in inclusive $e^+e^- \rightarrow J/\psi X$ events. The enhancements correspond to the η_c , χ_{c0} , $\eta_c(2S)$ and a new state, $X(3940)$. The curves are described in the text.

perform a fit to this spectrum that includes three known (η_c , χ_{c0} , $\eta_c(2S)$) and one new ($X(3940)$) charmonium states. In this fit, the mass positions for the η_c , χ_{c0} , $\eta_c(2S)$ and $X(3940)$ are free parameters. The expected signal line-shapes are determined from Monte Carlo (MC) simulation as described in the previous Belle publications [5, 6]. As the width of the new state is unknown, it is a free parameter in the fit. Thus the signal function for the $X(3940)$ is a convolution of the Monte Carlo line shape, with assumed zero width, with a Breit-Wigner function. The background is parametrized by a second order polynomial function and a threshold term ($\sqrt{M_{\text{recoil}}(J/\psi) - 2M_D}$) to account for a possible contribution from $e^+e^- \rightarrow J/\psi D^{(*)}\bar{D}^{(*)}$.

The fit results are given in Table I. The significance for each charmonium signal is defined as $\sqrt{-2 \ln(\mathcal{L}_0/\mathcal{L}_{\text{max}})}$, where \mathcal{L}_0 and \mathcal{L}_{max} denote the likelihoods returned by the fits with the signal yield fixed at zero and at the fitted value respectively for each charmonium state. The signal for the $X(3940)$ is found to have a significance of 5.0σ . The width of the $X(3940)$ state is consistent with zero, with a large statistical error: $\Gamma = 39 \pm 26 \text{ MeV}/c^2$. The fit results are shown in the Fig. 1 as the solid curve; the dashed curve is the background function.

The new state has a mass well above $D\bar{D}$ threshold. We therefore perform a search for $X(3940)$ decays into $D\bar{D}$ and $D^*\bar{D}$ final states. Because of the small product of $D^{(*)}$ reconstruction efficiencies and branching fractions, it is impossible to reconstruct fully the chain $e^+e^- \rightarrow J/\psi X(3940)$, $X(3940) \rightarrow D^{(*)}\bar{D}$. To increase the efficiency only one D meson in the event is reconstructed in addition to the reconstructed J/ψ . The other \bar{D} or \bar{D}^* can be detected as a peak in the spectrum of masses recoiling against the $J/\psi D$ combination. The Monte Carlo simulation for $e^+e^- \rightarrow J/\psi \bar{D}D$ and $e^+e^- \rightarrow J/\psi D^*\bar{D}$ processes predicts a $M_{\text{recoil}}(J/\psi D)$ resolution of about $30 \text{ MeV}/c^2$, thus the separation between these two processes is 2.5σ . Fig. 2 shows the $M_{\text{recoil}}(J/\psi D)$ spectrum in the D mass window

TABLE I: Summary of the signal yields, charmonium masses and significances for $e^+e^- \rightarrow J/\psi (c\bar{c})_{\text{res}}$.

$(c\bar{c})_{\text{res}}$	N	$M [\text{GeV}/c^2]$	σ
η_c	501 ± 44	2.970 ± 0.005	15.3
χ_{c0}	230 ± 40	3.406 ± 0.007	6.3
$\eta_c(2S)$	311 ± 42	3.626 ± 0.005	8.1
$X(3940)$	266 ± 63	3.936 ± 0.014	5.0

(points with error bars) and in the scaled D mass sidebands (hatched histogram), where D includes D^0 and D^+ . Two peaks around the nominal D and D^* masses are clearly visible in this distribution. The excess of real D events compared to the D sidebands at masses above $2.1 \text{ GeV}/c^2$ can be explained by $e^+e^- \rightarrow J/\psi D^* \bar{D}^*$ or $e^+e^- \rightarrow J/\psi D^{(*)} \bar{D}^{(*)} \pi$ processes. A fit to this spectrum is performed using shapes fixed from MC for three processes ($J/\psi D \bar{D}$, $J/\psi D^* \bar{D}$ and $J/\psi D^* \bar{D}^*$) and a second order polynomial function. The fit finds

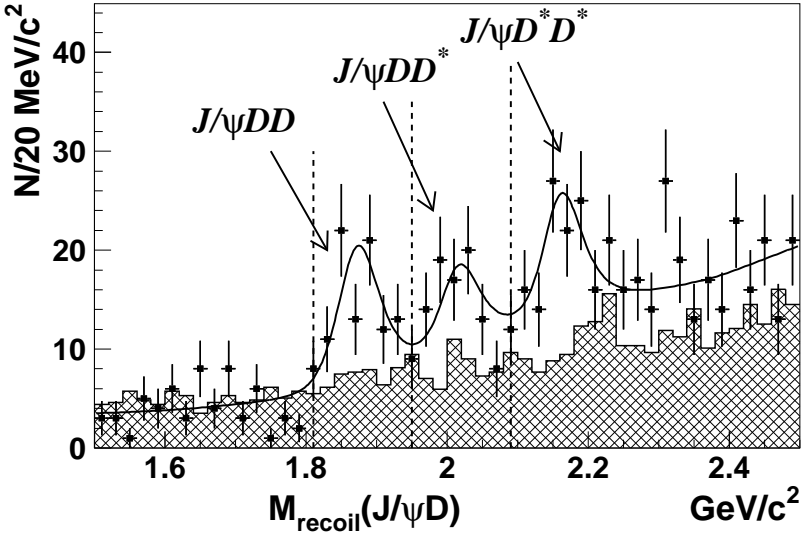


FIG. 2: The distribution of masses recoiling against the reconstructed $J/\psi D$ combinations in the data. The curve represents the fit, explained in the text.

$N_{DD} = 86 \pm 17$ (5.1σ) and $N_{D^*D} = 55 \pm 18$ (3.3σ) events in the D and the D^* peaks, respectively. Selecting the events from the $M_{\text{recoil}}(J/\psi D)$ regions around D and D^* masses ($\pm 70 \text{ MeV}/c^2$), we thus effectively tag the processes $e^+e^- \rightarrow J/\psi D \bar{D}$ and $e^+e^- \rightarrow J/\psi D^* \bar{D}$. Only one reconstructed $(J/\psi D)$ pair with the best mass fit to the nominal D mass in each region per event is accepted. Using additional information from the reconstructed D meson, we can improve the resolution of $M(D^{(*)}\bar{D}) \equiv M_{\text{recoil}}(J/\psi)$ by a factor of 2.5, according to the MC simulation. The $M_{\text{recoil}}(J/\psi D)$ is constrained to the nominal masses of D and D^* for two regions, respectively. Two possibilities exist in case of $X(3940)$ decays into $D^* \bar{D}$: the reconstructed D can be either from $X(3940)$ decays or from the D^* decay. In the latter case the constraint $M_{\text{recoil}}(J/\psi D) \rightarrow M(D^*)$ also works properly, as both $X(3940) \rightarrow D^* \bar{D}$

and D^* decay in a very restricted region of phase space.

The distribution of $M_{\text{recoil}}(J/\psi)$ after the kinematical constraint $M_{\text{recoil}}(J/\psi D) \rightarrow M(D)$ for a region of $M_{\text{recoil}}(J/\psi D)$ around $M(D)$ is shown in Fig. 3 a). The corresponding distribution for $e^+e^- \rightarrow J/\psi D^*\bar{D}$ is shown in Fig. 3 b). The cross-hatched histograms show the scaled D sideband distributions; in the sidebands a single candidate per event is selected closest in mass to the center of the sideband. A $X(3940)$ peak with a resolution better than

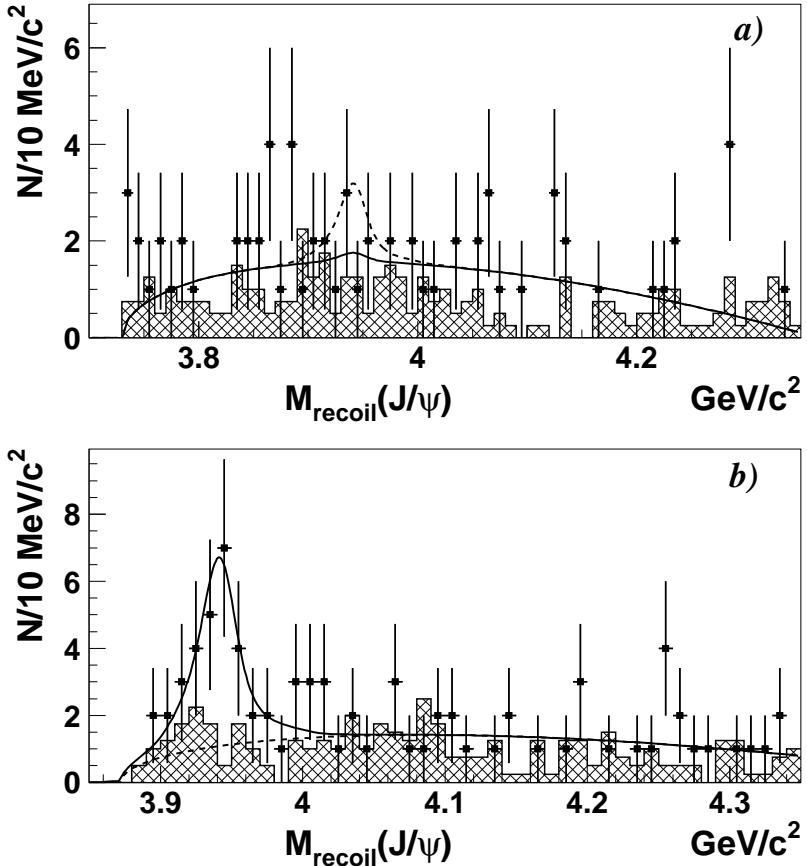


FIG. 3: The $M_{\text{recoil}}(J/\psi)$ distribution in the data: a) for events tagged and constrained as $e^+e^- \rightarrow J/\psi D\bar{D}$; b) for events tagged and constrained as $e^+e^- \rightarrow J/\psi D^*\bar{D}$. The hatched histograms correspond to scaled D sidebands. The solid lines are result of the fits, described in the text. The dotted lines show: a) the signal set at the value corresponding to the 90% C.L. upper limit; b) the background function.

in the unconstrained $M_{\text{recoil}}(J/\psi)$ distribution is evident in Fig. 3 b), corresponding to the decay $X(3940) \rightarrow D^*\bar{D}$. We perform a fit to this distribution. The signal function is a convolution of a Breit-Wigner with a free width and a resolution function fixed to the MC expectation (the core Gaussian has a width of $\sim 10 \text{ MeV}/c^2$). The background function is a threshold function $(A + B \cdot M(D^*\bar{D}))\sqrt{M(D^*\bar{D}) - M_{\text{thr}}}$ with $M_{\text{thr}} \equiv M(D^*) + M(D)$. The fit yields the number of signal events in the peak $N = 24.5 \pm 6.9$ with a significance of 5.0σ . The width of the $X(3940)$ is found to be $\Gamma = (15.4 \pm 10.1) \text{ MeV}/c^2$. The mass of the state is measured to be $M = 3.943 \pm 0.006 \text{ GeV}/c^2$.

We perform a similar fit to the $M_{\text{recoil}}(J/\psi)$ distribution for events tagged and constrained as $e^+e^- \rightarrow J/\psi D\bar{D}$. No $X(3940)$ signal is seen here, thus we fit this distribution with

TABLE II: Contribution to the systematic error for $\sigma_{\text{Born}}(e^+e^- \rightarrow J/\psi X(3940))$ and $\mathcal{B}(X(3940))$ [%].

Source	σ_{Born}	$\mathcal{B}(X(3940))$		
		$D^*\overline{D}$	$D\overline{D}$	$J/\psi\omega$
Fitting procedure	± 11	± 17	–	–
Angular distributions	± 19	± 12	± 12	± 16
N_{ch} cut	± 3	± 3	± 3	± 3
Reconstruction	± 2	± 6	± 6	± 5
Identification	± 3	± 1	± 1	–
Total	± 23	± 22	± 14	± 17

$X(3940)$ parameters fixed to the values found by the fit of tagged $e^+e^- \rightarrow J/\psi D^*\overline{D}$. The background function is $(A + B \cdot M(D\overline{D}))\sqrt{M(D\overline{D}) - 2 \cdot M(D)}$. The signal yield is found to be $0.2^{+4.4}_{-3.5}$ events and we set an upper limit for the $X(3940)$ signal to be smaller than 8.1 events at the 90% C.L.

An enhancement with a similar mass, $Y(3940)$, decaying into $J/\psi\omega$ has been recently observed by Belle [3] in B decays. We perform a search for the decay $X(3940) \rightarrow J/\psi\omega$ to check if $X(3940)$ and $Y(3940)$ could be the same particle. To increase the efficiency we reconstruct the ω and only one J/ψ from the $J/\psi J/\psi\omega$ final state. The unreconstructed J/ψ can be seen in the spectrum of recoil masses against the reconstructed $J/\psi\omega$ combinations. Two possibilities exist: the reconstructed J/ψ can be either prompt or from $X(3940)$ decays. There are correspondingly two possibilities to look for a signal of $X(3940) \rightarrow J/\psi\omega$: in the first case, the peak of $X(3940)$ should be seen in the distribution of $M_{\text{recoil}}(J/\psi) - M_{\text{recoil}}(J/\psi\omega) + M(J/\psi)$ around the nominal $X(3940)$ mass, in the second case $X(3940)$ peak appears in the $J/\psi\omega$ invariant mass distribution. The first case has much larger combinatorial background and less sensitivity, thus we use only the second case. The scatter plot of $M_{\text{recoil}}(J/\psi\omega)$ vs. $J/\psi\omega$ invariant mass in the data is shown in Fig. 4a). Two projections are shown in Fig. 4b) and c) after applying additional requirements: $|M_{\text{recoil}}(J/\psi\omega) - M_{J/\psi}| < 100 \text{ MeV}/c^2$ for the $M(J/\psi\omega)$ projection, and $|M(J/\psi\omega) - M_{X(3940)}| < 40 \text{ MeV}/c^2$ for the $M_{\text{recoil}}(J/\psi\omega)$ projection. The scaled ω mass sidebands are shown as hatched histograms. The fit to the $J/\psi\omega$ invariant mass distribution in Fig. 4b) is done with the signal function and parameters fixed from the result of the $D^*\overline{D}$ tagged fit; the background is a threshold function. The fit yields $1.9^{+3.2}_{-2.4}$ signal events corresponding to a 7.4 events upper limit at the 90% C.L. The fit to $M_{\text{recoil}}(J/\psi\omega)$ distribution yields $2.2^{+4.5}_{-3.7}$ events. In the latter fit the signal parametrization is fixed from the MC, and the background is a linear function.

The systematic errors for the $e^+e^- \rightarrow J/\psi X(3940)$ Born cross section and for the $X(3940)$ branching fractions $\mathcal{B}(X(3940))$ are summarized in Table II. To estimate the fitting systematics we study the difference in $X(3940)$ yield returned by the fit to the $M_{\text{recoil}}(J/\psi)$ distribution under different assumptions for the signal and background parametrization. In particular in the first fit we use a background function that includes several threshold functions corresponding to the production of $D^*\overline{D}$ and $D^*\overline{D}$. We also use the threshold function

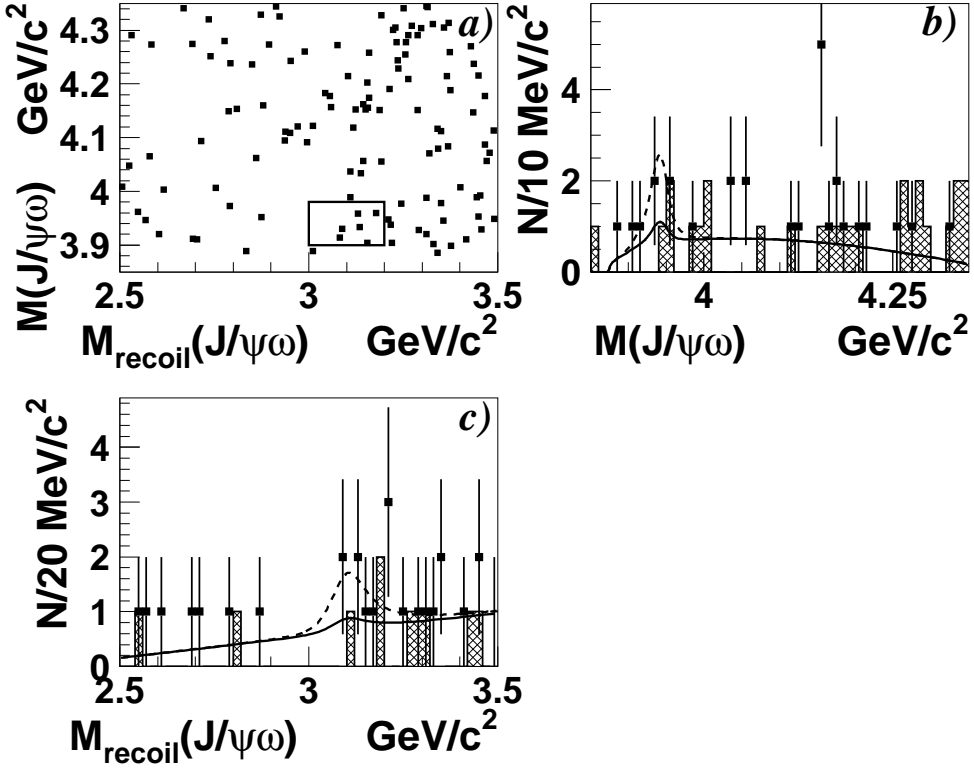


FIG. 4: a) The scatter plot of $M_{\text{recoil}}(J/\psi\omega)$ vs. $M(J/\psi\omega)$; b) the $M(J/\psi\omega)$ projection; and c) the $M_{\text{recoil}}(J/\psi\omega)$ projection. Points with errors bars show the contribution from the ω mass window; hatched histograms correspond to the ω sideband. The solid line represents the fit described in the text. The dotted lines correspond to the case where the contribution of $X(3940) \rightarrow J/\psi\omega$ is set at the 90% C.L. upper limit value.

$(A + B \cdot M_{\text{recoil}}(J/\psi))\sqrt{M_{\text{recoil}}(J/\psi) - M_{\text{thr}}}$. Different angular distributions result in different J/ψ (and D) reconstruction efficiencies. In the MC the J/ψ production angle and J/ψ , $X(3940)$ helicity angle distributions are assumed to be flat. The possible extreme angular distributions ($1 + \cos^2 \theta$ and $\sin^2 \theta$) are considered to estimate the systematic uncertainty of this assumption. This uncertainty is partially canceled out in the calculated $\mathcal{B}(X(3940))$ due to cancellation of the J/ψ efficiency. The systematics due to the $N_{\text{ch}} > 4$ cut is due to the unknown charged multiplicity in $X(3940)$ decays: the efficiency to pass this cut for 4-prong $X(3940)$ decay is about 96%, while this cut is 100% efficient for 6-prong decays. Other contributions come from the track reconstruction efficiency; lepton identification for reconstructed J/ψ and kaon identification for reconstructed D .

The systematic errors in the measurement of the $\eta_c(2S)$ and $X(3940)$ masses as well as the $X(3940)$ width are dominated by the fitting systematics. For $\eta_c(2S)$ the dominant uncertainty is due to the ISR that affects the signal parametrization. The uncertainty in the mass measurement of $X(3940)$ is dominated by the background parametrization; the signal function is known better as the ISR tail is significantly suppressed by the $D^*\overline{D}$ tagging and fitting procedure. Finally the fitting systematic errors are estimated to be $5 \text{ MeV}/c^2$ for both states. Another uncertainty exists due to the J/ψ momentum scale and was estimated in the previous paper [6] to be smaller than $3 \text{ MeV}/c^2$.

The Born cross section for $e^+e^- \rightarrow J/\psi X(3940)$ is calculated following the procedure used in the previous analysis [6]. The signal yield found by the fit is corrected by the reconstruction efficiency. As in the previous Belle papers, because of selection criteria the result is presented in terms of the product of the cross section and the branching fraction of the $X(3940)$ into more than 2 charged tracks ($\mathcal{B}_{>2}$). We obtain

$$\sigma_{\text{Born}} \times \mathcal{B}_{>2} = (10.6 \pm 2.5 \pm 2.4) \text{ pb.} \quad (2)$$

Using the $X(3940)$ yields in inclusive and $D^*\overline{D}$ tagged samples, we calculate $\mathcal{B}(X(3940) \rightarrow D^*\overline{D})$. To remove the correlation between the two samples we apply a veto on $D^*\overline{D}$ tagging in the inclusive sample. Correcting by the tagging and veto efficiencies obtained from MC, we find

$$\mathcal{B}(X(3940) \rightarrow D^*\overline{D}) = (96^{+45}_{-32} \pm 22)\%. \quad (3)$$

In the MC we assume that $\mathcal{B}(X(3940) \rightarrow D^{*0}\overline{D}^0) = \mathcal{B}(X(3940) \rightarrow D^{*+}D^-)$. We also calculate an upper limit for the decay of $X(3940)$ into non- $D^*\overline{D}$ final states:

$$\mathcal{B}_{\text{non-}D^*\overline{D}}(X(3940)) < 48\% \text{ at 90\% C.L.} \quad (4)$$

We set upper limits on the branching fractions of $X(3940) \rightarrow D\overline{D}$ and $X(3940) \rightarrow J/\psi\omega$, taking into account the estimated systematic errors:

$$\mathcal{B}(X(3940) \rightarrow D\overline{D}) < 41\% \text{ at 90\% C.L.}; \quad (5)$$

$$\mathcal{B}(X(3940) \rightarrow J/\psi\omega) < 26\% \text{ at 90\% C.L.} \quad (6)$$

In summary, we have observed a new charmonium state, $X(3940)$, produced in the process $e^+e^- \rightarrow J/\psi X(3940)$ with a Born cross section of $(10.6 \pm 2.5 \pm 2.4) \text{ pb}$. We have also observed the decay $X(3940) \rightarrow D^*\overline{D}$ to be the dominant decay mode with a measured branching fraction of $(96^{+45}_{-32} \pm 22)\%$. The mass of the new state is measured to be $(3.943 \pm 0.006 \pm 0.006) \text{ GeV}/c^2$ with a width smaller than $52 \text{ MeV}/c^2$ at 90% C.L. We set upper limits for the decay $X(3940) \rightarrow D\overline{D}$ and $X(3940) \rightarrow J/\psi\omega$ of less than 41% and 26% at 90% C.L., respectively. The mass of $\eta_c(2S)$ is measured to be $M = (3.626 \pm 0.005 \pm 0.006) \text{ GeV}/c^2$.

[1] S.K. Choi *et al.* (Belle Collaboration), Phys. Rev. Lett. **89**, 102001 (2002).
[2] S.K. Choi *et al.* (Belle Collaboration), Phys. Rev. Lett. **91**, 262001 (2003).
[3] S.K. Choi *et al.* (Belle Collaboration), Phys. Rev. Lett. **94**, 182002 (2005).
[4] K. Abe *et al.* (Belle Collaboration), BELLE-CONF-0439, ICHEP04-8-0685, hep-ex/0408116.
[5] K. Abe *et al.* (Belle Collaboration), Phys. Rev. Lett. **89**, 142001 (2002).
[6] K. Abe *et al.* (Belle Collaboration), Phys. Rev. **D70**, 071102 (2004).